Received: 12 February 2018 | Revised: 4 April 2018 | Accepted: 4 April 2018
DOI: 10.1002/ppap.201800030

FULL PAPER

PLASMA PROCESSES AND POLYMERS

Specificity of detection methods of nitrites and ozone in aqueous solutions activated by air plasma

Barbora Tarabová[1] | **Petr Lukeš**[2] | **Mário Janda**[1] | **Karol Hensel**[1] | **Libuša Šikurová**[3] | **Zdenko Machala**[1]

[1] Division of Environmental Physics, Faculty of Mathematics, Physics and Informatics, Comenius University, Mlynská dolina, 84248 Bratislava, Slovakia

[2] Institute of Plasma Physics of the CAS, v.v.i., Za Slovankou 3, 18200 Prague, Czech Republic

[3] Division of Biomedical Physics, Faculty of Mathematics, Physics and Informatics, Comenius University, Mlynská dolina, 84248 Bratislava, Slovakia

Correspondence
Barbora Tarabová, Division of Environmental Physics, Faculty of Mathematics, Physics and Informatics, Comenius University, Mlynská dolina, 84248 Bratislava, Slovakia.
Email: tarabova@fmph.uniba.sk

Funding information
Slovak Grant Agency VEGA, Grant number: 1/0419/18; European Cooperation in Science and Technology, Grant number: COST Action TD1208; Slovak Research and Development Agency, Grant number: APVV-0134-12; Ministry of Education, Youth and Sports of the Czech Republic, Grant number: COST LD 14080

Air transient spark (TS) discharge generates cold plasma, which is a rich source of reactive oxygen and nitrogen species (RONS). The gaseous products both in ambient air and air humidified by water electrospray (ES) are nitrogen oxides (NO and NO_2). The rotational and vibrational temperatures determined by optical emission spectroscopy (OES) are lower with water ES through the discharge than in ambient air, which reduces the formation of NO_x. The investigation of the specificity of Griess colorimetric assay for the detection of long-lived nitrites in plasma activated solutions confirms its accuracy by comparison with ion chromatography (IC) and excludes possible interferences with hydrogen peroxide by using the enzyme catalase. Examination of the specificity of the Indigo blue assay for ozone detection shows strong interferences with the peroxynitrite chemistry. Phenol as the chemical probe confirms that the TS air discharge produces no aqueous ozone.

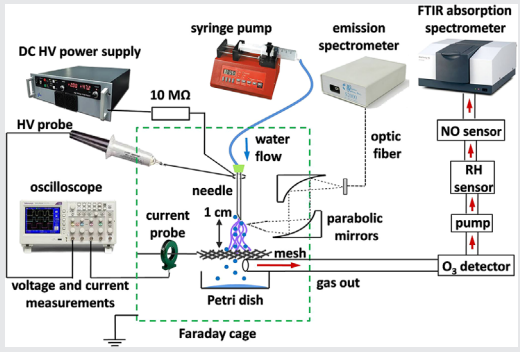

KEYWORDS
DC discharges, nitrites, ozone, plasma activated water, UV–VIS spectroscopy

1 | INTRODUCTION

Cold (non-thermal) plasmas generated by electrical discharges at atmospheric pressure have been extensively studied in recent years for their applications in biology, medicine, and agriculture. Their bio-relevant effects are especially due to the combination of several plasma agents such as electric field, UV radiation, or reactive species. Among these, neutral reactive species along with some ions probably play the dominant role in the sterilization, wound healing, skin diseases treatment, or potential cancer treatment induced by cold plasma.[1–6] Discharges generated in ambient air or in gases containing nitrogen and oxygen produce various reactive oxygen and nitrogen species (RONS), which may have different effects, for example, antibacterial/cytotoxic or therapeutic. The effects of cold plasma can also be mediated through so called *plasma activated water/solutions/media* (PAW/PAS/PAM),[7–12] which are formed during the plasma exposure of various aqueous solutions, for example, deionized water, physiological saline solution,

different buffered solutions, or cell cultivation media. Plasmas of various types of electrical discharges may be generated in a variety of set-ups and various gas mixtures interacting with liquids and affecting the solutions directly or indirectly.[13] Plasma treatment in general induces chemical changes in the activated solutions due to the plasma-chemical and transport processes occurring in and through the plasma-liquid interface. The plasma induced chemical changes in aqueous solutions depend on many parameters, such as the type of the discharge, its power, composition of the gas mixture, as well as composition and properties of used solutions. Electrical discharges generated at the gas-liquid interface induce formation of the gaseous reactive species (e.g., $O^{\bullet}$, $N^{\bullet}$, $H^{\bullet}$, $NO^{\bullet}$, $NO_2^{\bullet}$, $OH^{\bullet}$, H_2O_2, HNO_2, O_3). These can penetrate or dissolve through the gas-liquid interface into the liquids and further induce formation of the reactive species directly in the bulk liquid. RONS formed in the plasma activated aqueous solutions can be relatively long-lived (H_2O_2, NO_2^-/NO_3^-, O_3) or transient with very short life-times ($OH^{\bullet}$, $NO^{\bullet}$, $NO_2^{\bullet}$, ONOOH/$ONOO^-$, $HOO^{\bullet}/O_2^{\bullet -}$).[14,15]The properties of plasma activated solutions are time-variable, depending on pH and temperature, and their mutual reactivity. Therefore some of the PAS properties decay exponentially in post-discharge time.[9,11,16,17] For every application of plasma activated solution it is important to know their properties and limitations, which can only be determined by the accurate detection of every single RONS. However, the RONS detection may be often difficult due to their very short life-times, strong reactivity, low concentrations, etc.

In plasmas in ambient or synthetic air and nitrogen carrier gases, nitrogen oxides (NO_x) are typically formed in considerable amounts.[18–23] The NO_x generation in plasmas with aqueous solutions is also of interest due to their antibacterial ($NO_2^{\bullet}$) and biomedical ($NO^{\bullet}$, $NO_2^{\bullet}$) effects. Some plasma devices are designed to produce significant NO_x densities.[20,24–26] Nitrites NO_2^- (and nitrates NO_3^-) are formed in plasma activated solutions by the dissolution of nitrogen oxides from the gas phase and they are linked with the acidification of the solution. Furthermore, via peroxynitrite chemistry (ONOOH/$ONOO^-$ formation), their acidic decay, or in the presence of UVA photons,[27] nitrites participate at the production of biologically important radicals – $NO^{\bullet}$, $NO_2^{\bullet}$, and $OH^{\bullet}$, which are known for their antibacterial,[9,10,28] therapeutical,[2,29] or anti-cancer properties.[30] The most common method of nitrite detection in plasma activated solutions is a colorimetric Griess assay. It has been widely used in various aqueous solutions (deionized water, Milli Q water, saline solution, phosphate or citrate buffered solution, phosphate buffered saline) treated by different plasma sources (dielectric barrier discharge, plasma jets, gliding arc, spark discharge).[31–37] In the original Griess reaction (diazotation reaction), nitrite reacts with sulfanilic acid under acidic conditions to form a diazonium ion, which couples to α-naphthylamine to form a readily water-soluble, red-violet colored azo dye. The sulfanilic acid and α-naphthylamine are called the Griess reagents. Derivatives of these nitrosable and coupling components can be also used – sulfanilamide and N-(1-naphtyl)ethylenediamine.[38] Besides the Griess assay, other methods for nitrites detection can be used. Direct UV absorption in aqueous solutions for nitrites gives the absorption maxima at ~350–360 nm or 200–210 nm. The limitation of this method is the overlap of nitrites and nitrates bands at ~200 nm and relatively low sensitivity.[39,40] Ion/high performance liquid chromatography (HPLC) is a very precise and reliable method. Both direct UV absorption and ion chromatography (IC) have been used for nitrite detection in plasma activated solutions.[8,9,23,41–44]

Ozone is one of the abundant reactive species formed in air or oxygen plasma discharges with relatively low power, for example, pulsed corona discharge, dielectric barrier discharge, or low-power surface micro discharge.[18,42,45–47] Plasma jets can also generate O_3 when a small amount of oxygen is added into the carrier noble gas or when the ambient or synthetic air are used as shielding gases or are present in the surrounding gas atmosphere.[48,49] Ozone is formed in the gas phase and can dissolve into the liquids. It is a powerful oxidant and disinfectant, it has a high redox potential and can oxidize organic compounds in water, remove pollutants including pathogens, and remove odors.[50,51] Methods for the determination of the residual ozone in aqueous solutions are mostly based on the absorption spectroscopy. Indigo trisulfonate (Indigo blue) assay is a colorimetric method, which was set as a standard method for the residual ozone detection in water.[52,53] It has been well tested and applied for the determination of ozone in many different types of water. Indigo blue is a well known classical blue vat dye that in aqueous solutions absorbs light at ~600 nm with a rather high molar absorptivity. The indigo blue method utilizes the discolorization of the stock solution of blue indigo trisulfonate by dissolved ozone. Ozonolysis of the only one C═C bond in indigo blue produces sulfonated isatin and eliminates the absorbance of the aqueous solution. This method has been widely used for the dissolved ozone detection in plasma activated aqueous solutions.[37,42,47,54–58] Some authors used another sensitive spectrophotometric method, which was described in the edition of the Standards Methods – Iodometric method. Ozone reacts with the neutral potassium iodide solution and liberates iodine. In the excess of potassium iodide, iodine is in the complexed triiodide form. The concentration of triiodide is determined spectrophotometrically at 352 nm[52] and it was used in ref.[57,59–63] Furthermore, ozone can be very specifically detected by using phenol as a chemical probe and detecting its degradation product muconic acid.[9,64]

In this work we focused at the formation and detection of RONS induced by cold air plasma in the gas phase and in aqueous solutions. We analyzed the gaseous products formed by the positive transient spark (TS) discharge generated in ambient air and ambient air with water electrospray (ES) through the discharge and liquid RONS (hydrogen peroxide H_2O_2, nitrites NO_2^-, nitrates NO_3^-, and dissolved ozone O_3) in aqueous solutions electrosprayed through the discharge. We compared the accuracy of the Griess assay for nitrites detection with the ion chromatography method. We also evaluated the possible interferences of H_2O_2 on the specificity of Griess assay of nitrites by the addition of catalase. The specificity of the Indigo blue assay was investigated by using scavengers of RONS (catalase, mannitol, and sodium azide) and in synthetic PAW (sPAW), that is, chemical solution mimicking the PAW composition. Phenol degradation by TS ES was investigated in order to clarify the main chemical pathways in plasma activated solutions.

2 | EXPERIMENTAL SET-UP AND METHODS

2.1 | Transient spark with water electrospray

The experimental set-up of the water ES system[10] is depicted in Figure 1. A DC-driven TS discharge in positive polarity was generated in point-to-plane configuration in ambient air at atmospheric pressure. TS discharge is a self-pulsing repetitive streamer-to-spark discharge with very short duration (<50 ns) of spark current pulse (~20–30 A) with the typical repetitive frequency ~1 kHz and has been studied and described in detail in.[65–67] The reactor consisted of the high voltage (HV) hollow needle electrode which allowed for the injection of the aqueous solutions with the constant flow rate 0.5 mL min^{-1} by the syringe pump *Pump Systems NE-300* directly through the active discharge zone. Due to the applied HV on the needle, the effect of electro-spraying of solutions into fine micrometric size droplets occurred.[68,69] The needle nozzle with a special cut facilitates a better contact of the microdroplets of the sprayed solutions with the discharge. The inter-electrode spacing between the HV needle tip and the metallic grounded mesh was kept at 10 mm. A positive HV was applied through the ballast resistor R (10 MΩ). The discharge voltage was measured by the HV probe *Tektronix P6015A* and the discharge current was measured by a Rogowski current monitor *Pearson Electronics 2877*. The electrical parameters were processed and recorded during the experiments by a 200 MHz oscilloscope *Tektronix TDS 2024C*. Typical current and voltage waveform of TS discharge with ES, as well as electrical parameters, were documented in detail in our previous publications.[10,70]

2.2 | Chemical diagnostics of the gas-phase products

The experiments focused at the diagnostics of the gas-phase discharge products were carried out in the open reactor in ambient air. The analyzed gas was pumped through a tube placed directly below the grounded mesh electrode by the pump with the flow rate 0.5 L min^{-1}. Ozone concentrations were measured by a home-made ozone analyzer based on UV absorption at 254 nm and the Lambert-Beer law (absorption cross-section 1.15×10^{-21} m^2 at room temperature) with the gas cell length 12.5 cm.[71] NO was detected by the electrochemical gas sensor *Membrapor NO/SF-1000* with the resolution 5 ppm and the range up to 1000 ppm. Nitrogen oxides, ozone, and other gas molecules were detected by the Fourier transform infrared (FTIR) absorption spectrophotometer *Shimadzu IRAffinity-1S* inside the 10 cm long gas cell with the spectral resolution 0.5 cm^{-1}. NO_x concentrations were calculated according to the absorption maximum wavelengths 1900.36 cm^{-1} for NO and 1627.43 cm^{-1} for NO_2, after calibration with calibration standard NO and NO_2 gases in N_2 and air, respectively.

In order to discover more about reactive species generated by the TS discharge with and without the water ES, we performed a time-integrated optical emission spectroscopy (OES). The OES technique can provide valuable information on excited atomic and molecular states. It enables to determine the rotational, vibrational, and electronic excitation temperatures of the plasma and thus the level of non-equilibrium.[72–74] For fast recording of time-integrated spectra of a broad spectral region we used a two-channel compact emission spectrometer *Ocean Optics SD2000* (200–1100 nm, resolution 0.6–1.7 nm). Spectra were measured in the position right below the needle anode in ambient air with and without the water ES through the discharge zone. The measured spectra were compared with spectra of the N_2 second positive system (SPS) simulated by Specair[72] in order to determine rotational and vibrational temperatures of $N_2(C)$ species. The $N_2(C)$ rotational temperature was used as an indicator of the gas temperature.

2.3 | Chemical diagnostics of plasma activated aqueous solutions

Aqueous solutions with different initial pH and electrolytic conductivities σ were used in our experiments. They were prepared by the dissolution of different phosphate salts in deionized water to obtain solutions with the following properties:

- phosphate buffer (**PB**) – 2 mM and 0.1 M Na_2HPO_4/KH_2PO_4 aqueous solution (pH 6.9, $\sigma = 560$ μS cm^{-1}) was used to control the pH of plasma activated solutions;

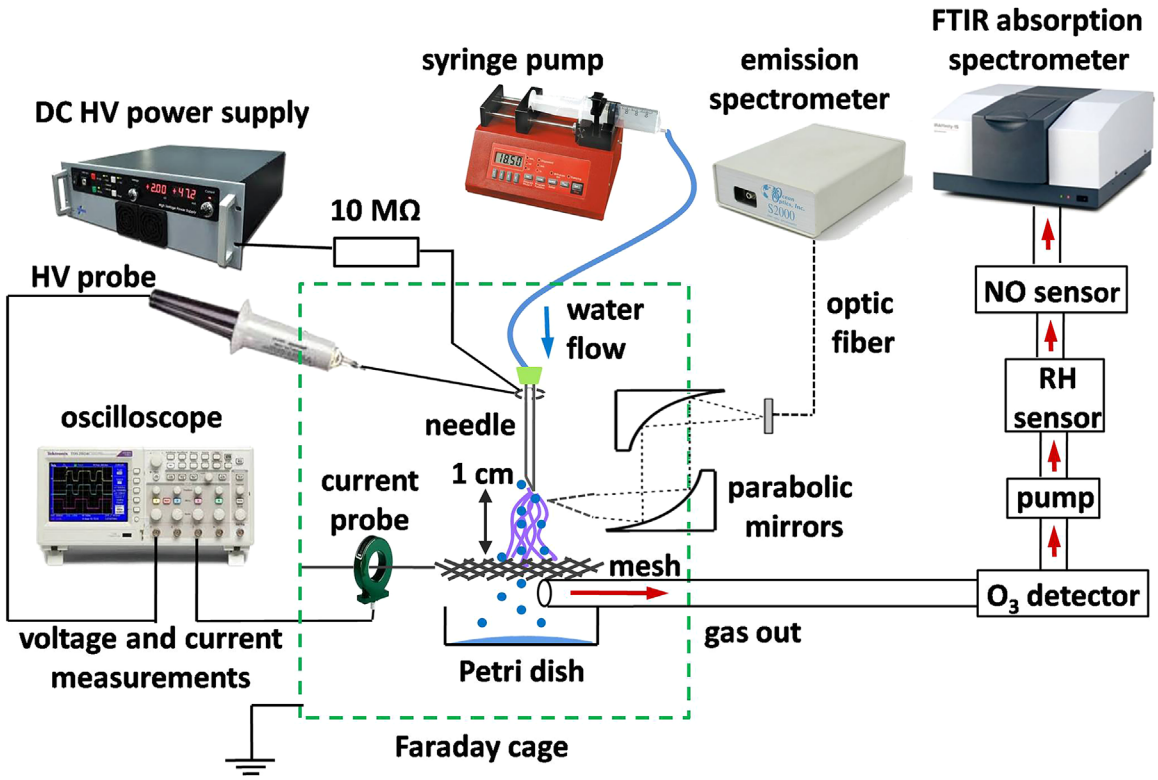

FIGURE 1 Experimental set-up of air transient spark discharge with water electrospray, optical emission spectroscopy, and analysis of gaseous products

- water (**W**) – NaH_2PO_4 solution (pH 5.5, $\sigma = 600\ \mu S\ cm^{-1}$) mimics the conductivity of tap water and has a similar chemical composition with the phosphate buffer;
- synthetic plasma-activated water (**sPAW**) – a mixture of 800 µM H_2O_2/400 µM $NaNO_2$ in phosphoric acid/NaH_2PO_4 solution (pH ~ 3.2) – simulates the typical chemical composition (pH, H_2O_2, and NO_2^- concentrations) of PAW.

The concentrations of RONS formed in plasma activated solutions due to the gas-liquid interactions were primarily detected by the colorimetric methods (UV/VIS absorption spectrophotometer *UV-1800 Shimadzu*). Additionally, comparative methods such as IC, and HPLC were used. Measurement of hydrogen peroxide was performed by the titanium oxysulfate assay. The principle of this method is a reaction of H_2O_2 with the titanium (IV) ions under acidic conditions. The yellow-colored product of pertitanic acid H_2TiO_4 is formed with the absorption maximum at 407 nm.[75] The concentration of H_2O_2 is proportional to the absorbance according to the Lambert-Beer's law (molar extinction coefficient $\varepsilon = 6.89 \times 10^2\ L\ .\ mol^{-1}\ .\ cm^{-1}$). Because of the possible H_2O_2 decomposition by NO_2^- under acidic conditions, sodium azide (60 mM) was added to the sample prior to mixing with the titanium oxysulfate reagent.[9] Sodium azide immediately reduces nitrites into molecular nitrogen and preserves the H_2O_2 concentration intact (Equation 1):

$$3\ N_3^- + NO_2^- + 4\ H^+ \rightarrow 5\ N_2 + 2\ H_2O \qquad (1)$$

Griess assay is a well known and selective method for nitrite detection.[38] It was also set as a standardized method for the examination of water and wastewater.[52] This colorimetric method is based on the reaction of NO_2^- with the Griess reagents under acidic conditions, which after their reaction convert into deep purple azo compound with the absorption maximum at 540 nm. In this work we used two different Griess assays. The first assay contained the Griess reagents prepared according to *Method 4500–NO_2^-* in ref.[52] The second assay was *Nitrate/Nitrite Colorimetric Assay Kit* (# 780001, Cayman Chemicals) that contained already prepared ready-to-use Griess reagents. The main differences between these assays were the mixing sample/reagents ratio and the time necessary for the development of the colored product. We performed calibrations for the exact quantification of NO_2^- for both assays. Furthermore, we used IC for both nitrites and nitrates detection. Samples for IC analysis were stabilized by phosphate buffer (pH 6.9) immediately after being withdrawn from the plasma

activated solutions to stop the acidic decomposition of NO_2^- and their loss via the peroxynitrites formation that will be discussed later (Equations 16 and 18). Stabilized samples were then injected into the chromatography column. The concentrations were measured by the HPLC system *Shimadzu* LC-10A*vp* with UV (210 nm) and suppressed conductivity detection. Analyses were made by means of a 7-μm Allsep A1 anion exchange column (10 × 4.6 mm) with 0.85 mM $NaHCO_3$/0.9 mM Na_2CO_3 as the eluent (flow rate of 1.2 mL min^{-1}). The detection limit for analysis of NO_2^- and NO_3^- was 0.25 μM. In addition, Griess assays and IC were tested in combination with the enzyme catalase (*Catalase from bovine liver*, Sigma–Aldrich) to decompose H_2O_2 which may have a negative effect on the nitrite detection due to its participation in the peroxynitrite chemistry in PAW. Catalase is an intracellular enzyme which catalyzes the decomposition of H_2O_2 to water and oxygen (Equation 2):

$$2\ H_2O_2 \rightarrow 2\ H_2O + O_2 \quad (2)$$

The working solution of catalase with the activity 10.6 units mL^{-1} was prepared in 50 mM K_2HPO_4 buffer and it was mixed with the sample prior to mixing with the Griess reagents or prior the IC analysis.

The detection of the dissolved ozone in plasma activated solutions was performed by the Indigo blue assay. It is a simple and quantitative colorimetric standardized method for ozone detection (*Method 4500-O_3*) in water and wastewater,[52] which was developed by *Hoigné and Bader*.[53] In acidic conditions O_3 rapidly decolorizes the indigo potassium trisulfonate dye and the colorless product isatin is formed by the bleaching process. The decrease of the absorbance at 600 nm ($\varepsilon = 2.38 \times 10^4\ M^{-1}\ cm^{-1}$) is linear with the increasing concentration of dissolved O_3. We used indigo reagent II recommended for higher concentrations of O_3 (0.05-0.5 mg L^{-1}). It is important to find the best mixing ratio of the sample with indigo reagent, so that the solution will be still slightly colored. The ratio in our experiments was determined to be 1:1. We prevented the possible interferences with chlorine by using only non-saline solutions. H_2O_2 decolorizes the indigo blue reagent very slowly and does not interfere if O_3 is measured in less than 6 h. Nevertheless, we recorded the absorbance detection of samples within a few minutes after mixing with reagent. For the investigation of the specificity of this method, we also used scavengers of the key reactive species of the peroxynitrite formation – catalase (CAT) for H_2O_2 and sodium azide (SA) for NO_2^- scavenging, as well as mannitol (MAN) as a scavenger of $OH^\bullet$ radicals.

The detection of phenol and its degradation by-products by HPLC was used as an indirect analytical method to characterize the reactive pathways of RONS, especially of the dissolved O_3.[9] The specific chemical products of these pathways were detected after direct ES treatment of the 500 μM phenol solution by HPLC system *Shimadzu* LC-10 A*vp* with UV and fluorescence detection. Analyses were made using a 5 μM reversed phase Supelcosil LC-18 column (25 × 2.4 mm; Supelco). An isocratic method with a solvent mixture of 10% acetonitrile and 0.5% acetic acid in deionized water was used as the eluent with a flow rate 0.4 mL min^{-1}. The UV detection was performed at 250, 264, 274, 290, 320, and 350 nm. The fluorescence detection was made with the excitation and emission wavelengths of 271 and 297 nm, respectively. The detection limit for the HPLC analysis was 0.01–0.1 μM (depending on the compound and the used detection).

3 | RESULTS AND DISCUSSION

3.1 | Gas-phase products

Positive TS discharge was operated in ambient air at atmospheric pressure. The stable gaseous reactive species were identified both in the ambient air and in the ambient air humidified by the water ES through the discharge. The dominant stable gas phase products in ambient air were nitrogen oxides (NO and NO_2), while ozone was not detected (<10 ppm detection limit).

TS is a streamer-to-spark transition discharge initiated by a streamer which is followed by a nanosecond (<50 ns) spark pulse. During the rising slope of the current pulses (both streamer and spark), electrons have enough energy (temperature) to ionize dominant air molecules (N_2 and O_2) (Equations 3 and 4) and form the excited N_2* molecules (Equation 5):

$$e + N_2 \rightarrow e + e + N_2^+ \quad (3)$$

$$e + O_2 \rightarrow e + e + O_2^+ \quad (4)$$

$$e + N_2 \rightarrow e + N_2^*(N_2(C)\ \text{or}\ N_2(B)) \quad (5)$$

Fast quenching of the excited N_2* molecules with molecular oxygen is one of the sources of atomic oxygen (Equation 6)[76]:

$$N_2^* + O_2 \rightarrow N_2 + O + O \quad (6)$$

Although after the drop of the spark current pulses the electron temperature T_e decreases, electrons with lower energy still participate at the production of atomic O and N via their dissociative recombination with N_2^+ and O_2^+ ions (Equations 7 and 8):

$$e + O_2^+ \rightarrow O + O \ \left(O(^1D), (O(^1S)\right) \quad (7)$$

$$e + N_2^+ \rightarrow N + N \ \left(N(^2D), (N(^2P)\right) \quad (8)$$

Products of these reactions (Equation 6–8) may enhance the NO_x synthesis, especially due to N production, which helps to bypass the rate limiting step of the Zeldovich mechanism (Equations 9 and 10):

$$N + O_2 \rightarrow NO + O \quad (9)$$

$$O + N_2 \rightarrow NO + N \quad (10)$$

The dissociative recombination reactions (Equations 7 and 8) probably enhance the production of atomic oxygen species O, which results into the further oxidation of NO into NO_2 in a three-body reaction (Equation 11):

$$NO + O + M \rightarrow NO_2 + M \quad (11)$$

Furthermore, O atoms may also generate ozone O_3 (Equation 12), which is able to oxidize NO to NO_2 (Equation 13):

$$O + O_2 + M \rightarrow O_3 + M \quad (12)$$

$$O_3 + NO \rightarrow O_2 + NO_2 \quad (13)$$

However, there is a relatively high temperature during the spark pulse and ozone generated during the streamer-to-spark transition phase should be thermally decomposed and so the Zeldovich mechanism enhanced (Equations 9 and 10).[20] These plasma-chemical processes explain the formation of the dominant stable NO_x species and negligible O_3 formation in the TS plasma gas.

Figure 2 shows the concentrations of NO and NO_2 generated in the ambient air without (TS) and with ES (TS + ES). The ES of aqueous solutions through the plasma increases the interfacial surface of electrosprayed micrometric droplets and so improves the gas-liquid transport of the gaseous reactive species into the liquid. The enhanced NO_x dissolution into the electrosprayed water microdroplets depleted NO_x from the air. Figure 3 shows the emission spectra of TS with and without water ES with the determined rotational T_r and vibrational T_v temperatures. The uncertainties of the determined rotational and vibrational temperatures were approximately 100 and 250 K, respectively. Both T_r and T_v were lower in experiments with ES of water. Since T_r is close to the gas temperature T_g, we can see that the water ES cools down T_g from ~700 to ~400 K. Furthermore, we observed that the TS discharge with electrosprayed water

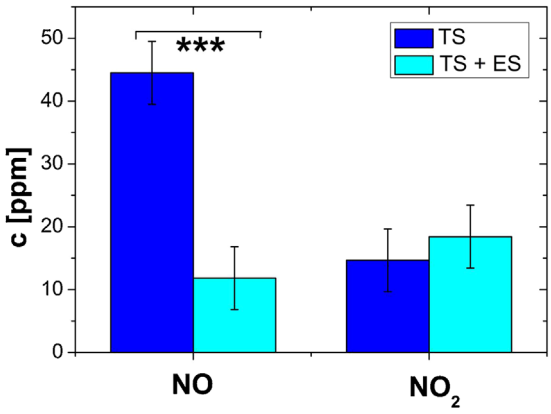

FIGURE 2 Nitrogen oxides (NO and NO_2) concentrations produced by transient spark discharge at ambient air with (TS + ES) and without (TS) water electrospray (mean ± SEM, n (TS) = 6, n (TS + ES) = 17); ***significant difference $p < 0.0001$ (Mann–Whitney test)

occupied larger volume and thus lower energy per unit volume was deposited into the gas. Therefore NO_x formation decreased due to the cooling by water and larger discharge volume and thus NO concentrations were found lower in the ES humidified air by the water ES. However, the NO_2 concentrations in the ES humidified air were measured approximately the same (within the experimental error). This is counter-intuitive and further investigation is needed.

3.2 | PAW chemistry with a focus at nitrite detection

TS discharge generated in ambient air was in the direct contact with the aqueous solutions electrosprayed directly

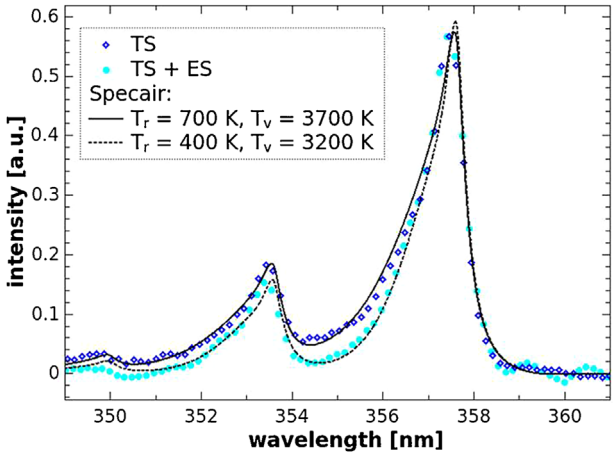

FIGURE 3 Emission spectra of TS discharge (~1 kHz) with (TS + ES) and without (TS) water electrospray, detail of N_2 SPS (0–1) and (1–2) bands. The simulated spectra with determined T_r and T_v for TS (black solid line) and TS + ES (black dashed line) were obtained using Specair software[72]

through the discharge. This cold air plasma activation resulted in the chemical effects induced in aqueous solutions. Changes of pH, conductivity, and formation of RONS were observed in water or PB and concentrations of hydrogen peroxide, nitrites, and nitrates were measured by titanium oxysulfate assay (H_2O_2) and IC (NO_2^-/NO_3^-). In both solutions (W and PB) the increase of conductivity was observed. In PAW the pH decreased ($5 \rightarrow 3.2$) unlike in plasma activated buffered solution (PAPB), where pH remained at 6.9. Figure 4 shows concentrations of H_2O_2, NO_3^-, and NO_2^- determined in PAW and PAPB solutions after TS ES treatment. Their concentrations depend on the pH of the solution.

Dissolution of gaseous NO_x along with the formation of NO_2^- and NO_3^- was responsible for the acidification of the plasma activated solutions (Equations 14 and 15):

$$NO_{2(aq)} + NO_{2(aq)} + H_2O_{(l)} \rightarrow NO_2^- + NO_3^- + 2\,H^+ \quad (14)$$

$$NO_{(aq)} + NO_{2(aq)} + H_2O_{(l)} \rightarrow 2\,NO_2^- + 2\,H^+ \quad (15)$$

The following processes are mainly responsible for the different concentrations of nitrites in PAW and PAPB:

1. Nitrites are not stable and decompose under acidic conditions (pH < 3.5) via formation of $NO^\bullet$ and $NO_2^\bullet$ intermediates (Equation 16) into nitrates as final products (Equation 17). $NO^\bullet$ and $NO_2^\bullet$ posses strong cytotoxic effects (also known as acidified nitrites)[77]

$$2\,NO_2^- + 2\,H^+ \leftrightarrow 2HNO_2 \rightarrow NO^\cdot + NO_2^\cdot + H_2O \quad (16)$$

$$2\,NO_2^\cdot + H_2O + H_2O \rightarrow NO_2^- + NO_3^- + H^+ \quad (17)$$

2. Nitrites can react with H_2O_2 in acidic environment and lead to the formation of peroxynitrites (peroxynitrous acid) (Equation 18), which are also very reactive through their decay products $OH^\bullet$ and $NO_2^\bullet$ radicals (Equation 19)[9,10,19,41,78]

$$NO_2^- + H_2O_2 + H^+ \rightarrow O{=}NOOH + H_2O \quad (18)$$

$$O{=}NOOH + OH^\cdot + NO_2^\cdot \quad (19)$$

Figure 5 shows the time evolution of the measured concentrations of long-lived species such as H_2O_2, NO_2^-, and NO_3^- in PAW in post plasma treatment time. The changes of their concentrations (decrease of H_2O_2 and NO_2^-, increase of NO_3^-) in time result from the ongoing post-discharge chemistry: particularly the above mentioned acidic decomposition of nitrites and formation of peroxynitrites. Furthermore, there are other reactions which may yield nitrite and nitrate ions, such as hydrolysis of $NO_2^\bullet$ or a reaction of $NO^\bullet$, and $NO_2^\bullet$ with dissolved oxygen.[9]

Since nitrites are one of the key and relatively stable species formed in plasma activated solutions, their detection is needful. As mentioned before, Griess assay is a specific method for NO_2^- detection based on colorimetric principle and it is easy to perform. Therefore we tested the accuracy of the Griess assay by the comparison with IC as a control method. Two different Griess reagents: Griess 1 prepared according to[52] and Griess 2 (*Nitrate/Nitrite Colorimetric Assay Kit*) were tested. In addition, we evaluated the effect of H_2O_2 on the specificity of Griess assay by addition of the catalase (CAT) enzyme to decompose H_2O_2 that may interfere the nitrite detection due to the fact that NO_2^- may also react with H_2O_2 through reaction (Equation 18) under the acidic conditions of Griess assay. Both solutions, W and PB were activated by the TS discharge with electrospray. Directly after treatment each sample was divided and the analysis of nitrites by IC, Griess 1, and Griess 2 (with or without added catalase) was performed.

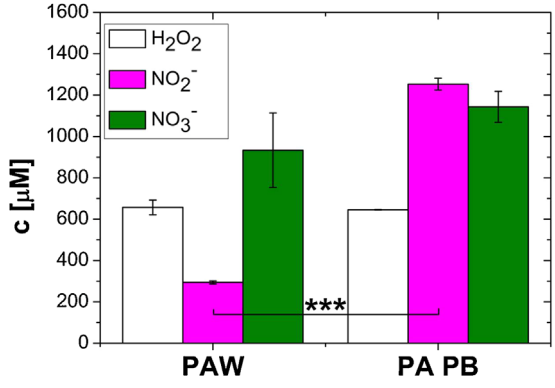

FIGURE 4 H_2O_2, NO_2^-, and NO_3^- (NO_2^-, NO_3^- measured by IC) concentrations in PAW and PAPB after electrospraying the W and PB solutions through transient spark (mean ± SEM, $n = 3$); ***significant difference $p < 0.0001$ (unpaired t-test)

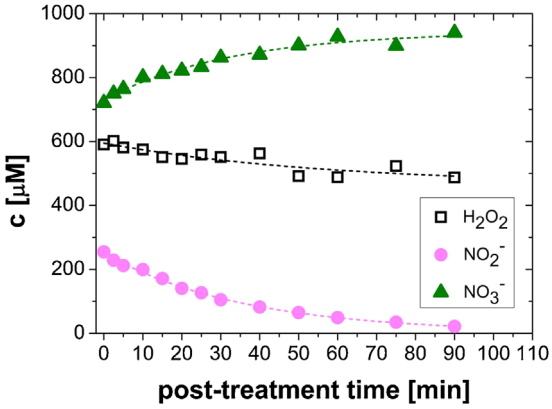

FIGURE 5 Evolution of H_2O_2, NO_2^-, and NO_3^- (NO_2^-, NO_3^- measured by IC) concentrations in PAW in post plasma treatment time

The measured NO_2^- concentrations for all cases are shown in Figure 6. The results of the NO_2^- detection by all three methods showed no significant difference between the samples with or without the added CAT. It seems that the reaction of Griess reagents with NO_2^- is faster than the competing reaction of H_2O_2 with NO_2^-. Also, due to the dilution of the treated samples for the Griess assay analysis (necessary to keep the nitrites concentrations in the linear part of the calibration curve), the concentration of H_2O_2 in the analyzed sample was 10–40 times lower which was sufficient to eliminate possible interferences of H_2O_2 on the analysis of NO_2^- by Griess assay. Moreover, the dilution of samples increased the pH, which slowed down or ceased the processes responsible for the nitrite decomposition (Equations 16 and 18). The comparison of the measured NO_2^- concentrations by two different Griess assays (Griess 1 and Griess 2) and by IC showed no significant differences. Following these results, we confirmed that the Griess assay is a precise, reliable and suitable method for the nitrite detection in plasma activated solutions.

3.3 | Dissolved ozone detection by the Indigo blue assay

Ozone dissolved in aqueous solutions is considered as very efficient oxidant and antimicrobial agent. Therefore we tried to detect the dissolved ozone in W treated by TS discharge with ES. By the Indigo blue method, we previously detected the concentrations about 2.5 mg L^{-1} (52 μM) of dissolved O_3 in the PAW.[79] Because TS discharge treatment decolorized the indigo blue dye even though there was no ozone detected in the gas phase, we verified the specificity of the indigo blue assay by using the simulated plasma activated water (sPAW), that is, the solution with similar chemical composition and pH as our typical PAW prepared by air TS discharge. Figure 7 shows the "apparent O_3" detected by the indigo blue assay by the same manner in post plasma treatment time in PAW, PAPB, and sPAW. The strong decolorization of the indigo blue dye was observed in PAW unlike in PAPB (0.1 M), where no decolorization was observed. The main difference between the PAW and PAPB are the plasma induced chemical changes due to the formation of RONS. The chemical changes differ depending on pH of the plasma treated solution. In the PAPB, where pH remained non-acidified (~6.9), the concentrations of H_2O_2 and NO_2^- were time-stable and the pH-dependent decomposition of nitrites (Equation 16) and peroxynitrite formation (Equation 18) did not occur. On the other hand, in acidified PAW (pH 3.2) these reactions (Equations 16 and 18) took place (Figure 5) and furthermore the acidic decomposition of peroxynitrites (Equation 19) into $OH^\bullet$ and $NO_2^\bullet$ radicals occurred.

The time evolution of "apparent O_3" in the sPAW was observed identical to PAW, despite the fact, that this solution was not in any contact with plasma and therefore no ozone could have been present. In sPAW, which contains only H_2O_2 and NO_2^- at acidic pH, only peroxynitrite formation occurred, followed by its immediate decomposition. The results show that the decolorization of the indigo blue dye in PAW and sPAW was almost the same despite no O_3 present in sPAW at all, and no O_3 was detected in the gas phase of TS discharge. We can thus assume that the Indigo blue decolorization in both these solutions without ozone (PAW and sPAW) was most likely caused by the hydroxyl radical $OH^\bullet$ formed as a decay product of peroxynitrites. This was probably also the reason for the false positive response of the Indigo blue dye method in PAW in our previous experiments.

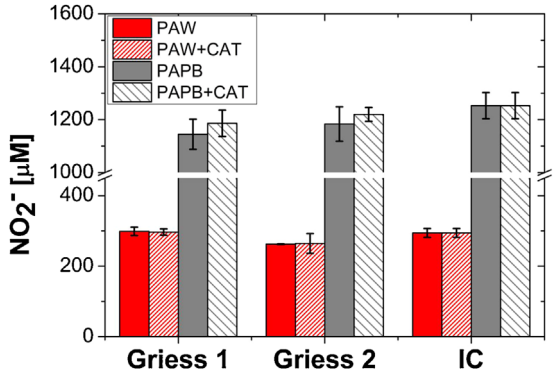

FIGURE 6 Comparison of the nitrite concentrations (mean ± SEM, $n = 3$) in PAW and PAPB measured by Griess assay 1, Griess assay 2, and by ion chromatography (IC) (with (+CAT) and without added catalase (scavenger of H_2O_2); no significant difference between each group Griess1, Griess 2, and IC for PAW and PAPB (Kruskal–Wallis test); no significant difference between PAW and PAPB with or without added catalase for each group (unpaired t-test)

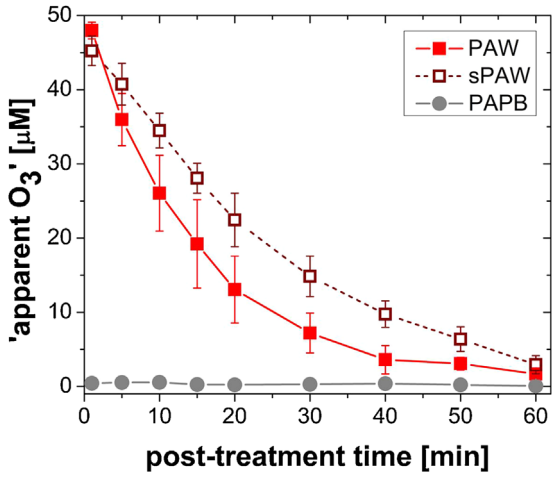

FIGURE 7 Evolution of the "apparent O_3" concentrations (mean ± SEM, $n = 3$) in post plasma treatment time in PAW, PAPB, and sPAW

In order to prove this hypothesis, we used the scavengers of certain reactive species with PAW and sPAW: catalase (CAT) to scavenge H_2O_2 (40 units mL^{-1}), sodium azide (SA) for NO_2^- (80 mM) and mannitol (MAN) for $OH^•$ radicals (100 mM). Both catalase and sodium azide were added into sPAW at the beginning of the analysis and mannitol was added into W before plasma treatment. Figure 8 shows how the addition of scavengers affected the decolorization of the indigo blue, and thus the detection of the "apparent ozone." Scavenging of the key reactants necessary for the peroxynitrite formation (H_2O_2 an NO_2^-) in sPAW decreased the decolorization of the indigo blue dye. Furthermore, mannitol scavenging the $OH^•$ radicals as the main product of peroxynitrite decay in PAW reduced the indigo blue decolorization too. Based on these results we confirmed that the Indigo blue assay for the detection of dissolved ozone is not suitable for the plasma activated water due to the strong interference with peroxynitrite chemistry occurring in PAW. It is noticeable, that *Anderson et al.*[33] observed the same results showing that air plasma inducing the peroxynitrite chemistry in plasma activated solutions significantly contributed to the decolorization of a similar indigo carmine dye due to the formation of $OH^•$ as a decay product in acidified PAW and sPAW.

In order to further analyze RONS in plasma activated solutions, phenol was used as chemical probe to characterize the specific primary products of its degradation by the reactive species formed during the plasma treatment in aqueous solutions. Phenol is a suitable model of organic compound and its reactions give specific degradation by-products after reaction with $OH^•$ radical, $NO^•$, and $NO_2^•$ radicals and especially with O_3.[9] Five hundred micrometer phenol solution prepared in W or PB (2 mM) was treated directly

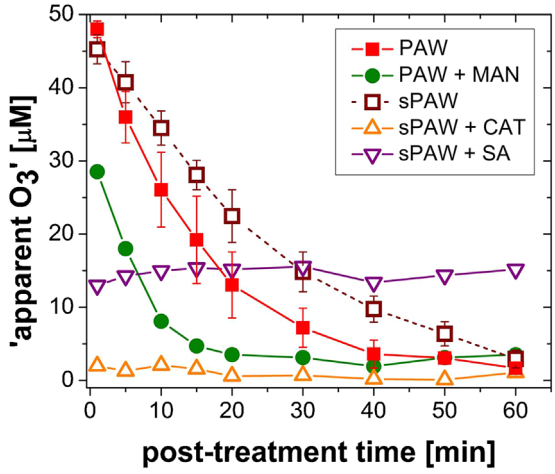

FIGURE 8 The effect of the scavengers on the "apparent O_3" concentrations (mean ± SEM, $n = 3$) in post plasma treatment time in PAW and sPAW with or without added scavengers. Used scavengers: MAN = mannitol (scavenger of $OH^•$); CAT = catalase (scavenger of H_2O_2); SA = sodium azide (scavenger of NO_2^-)

TABLE 1 Summary of the degradation by-products of phenol in PAW and PAPB

Phenol decomposition		PAW	PAPB
Phenol [μM]	Initial concentration	500	500
	After plasma treatment	297.3	309.3
	Decomposed	203	191
Hydroxylated products	Catechol Benzoquinone Hydroquinone Hydroxybenzoquinone	13% (26 μM)	11% (21 μM)
Nitrated products	4-nitrocatechol 2-nitrohydroquinone 4-nitrophenol 2-nitrophenol	5% (11 μM)	1% (2 μM)
'Ring-cleavage by O_3' products	*cis*, *cis*-muconic acid *cis*, *trans*-muconic acid	0	0

by the TS discharge with ES. The concentrations of residual phenol and its degradation products were analyzed using HPLC and the results are shown in Table 1. In PAW and PAPB solutions treated by the TS with ES, only the hydroxylated degradation products (catechol, hydroquinone, 1,4-benzoquinone, hydroxy-1,4-benzoquinone) and nitrated/nitrosylated by-products (4-nitrocatechol, 2-nitrohydroquinone, 4-nitrophenol, 2-nitrophenol) were detected, but no *cis, cis*-muconic acid (and its *cis, trans*-isomer) as a specific product of the ring cleavage of phenol by ozone. Contrary to the "apparent ozone" detected by the Indigo blue assay, the results from the phenol degradation product analysis showed no muconic acid and therefore no dissolved ozone in our air TS activated solutions. Even if some negligible ozone concentrations would be present in PAW, ozone would rapidly oxidize nitrites to nitrates and oxygen (Equation 20)[14]:

$$NO_2^- + O_3 \rightarrow NO_3^- + O_2 \qquad (20)$$

Moreover, the presence of hydroxylated and nitrated/nitrosylated by-products is an indirect evidence of the presence of both RONS: peroxynitrites and their decay products in acidic pH – $OH^•$ and $NO_2^•$ radicals, and also acidified nitrites. This result supports our previous evidence that the Indigo blue method is not specific to ozone detection in plasma activated solutions and strong peroxynitrite chemistry is responsible for the false ozone signal.

4 | CONCLUSION

Cold air plasmas produce a number of reactive species which act as antimicrobial agents and serve as precursors of RONS formed in plasma activated solutions that determine their antimicrobial and other properties. In this work, we showed

that the TS discharge generated in ambient air is a great source of nitrogen oxides: NO and NO_2. The ES of various aqueous solutions through the discharge enhanced the dissolution of these gaseous NO_x into the treated liquids, which induced formation of nitrites and nitrates and was linked with the acidification. Ozone was not detected in the gas phase due to its thermal decomposition during the spark phase. The time-averaged OES of N_2 second positive system was applied to determine the gas temperature and showed that the water ES decreased the gas temperature in the discharge. We showed that Griess assay is suitable for nitrite detection in plasma activated solutions and that H_2O_2 did not affect their detection. On the other hand, we showed that Indigo blue assay is strongly affected by $OH^{\bullet}$ radicals formed due to the acidic decay of peroxynitrites in the plasma activated solutions and therefore is not specific for ozone detection.

ORCID

Barbora Tarabová http://orcid.org/0000-0001-9936-1786
Petr Lukeš http://orcid.org/0000-0002-7330-0456
Mário Janda http://orcid.org/0000-0001-9051-4221
Karol Hensel http://orcid.org/0000-0001-6833-681X
Libuša Šikurová http://orcid.org/0000-0002-8825-7219
Zdenko Machala http://orcid.org/0000-0003-1424-1350

REFERENCES

[1] H. Tanaka, K. Ishikawa, M. Mizuno, S. Toyokuni, H. Kajiyama, F. Kikkawa, H.-R. Metelmann, M. Hori, *Rev. Mod. Plasma Phys.* **2017**, *1*, 3.
[2] C. V. Suschek, C. Opländer, *Clin. Plasma Med.* **2016**, 4.
[3] M. G. Kong, G. Kroesen, G. Morfill, T. Nosenko, T. Shimizu, J. van Dijk, J. L. Zimmermann, *New J. Phys.* **2009**, *11*, 115012.
[4] M. Ito, J.-S. Oh, T. Ohta, M. Shiratani, M. Hori, *Plasma Process. Polym.* **2017**, 1700073.
[5] R. Thirumdas, C. Sarangapani, U. S. Annapure, *Food Biophys.* **2015**, *10*, 1.
[6] M. Keidar, *Plasma Sources Sci. Technol.* **2015**, *24*, 33001.
[7] P. Lu, D. Boehm, P. Bourke, P. J. Cullen, *Plasma Process. Polym.* **2017**, e1600207.
[8] A. Kojtari, UK Ercan, J. Smith, G. Friedman, R. B. Sensening, S. Tyagi, S. G. Joshi, H-F. Ji, A. D. Brooks, *J. Nanomedine. Biotherapeutic Discov.* **2013**, *4*, 1.
[9] P. Lukes, E. Dolezalova, I. Sisrova, M. Clupek, *Plasma Sources Sci. Technol* **2014**, *23*, 15019.
[10] Z. Machala, B. Tarabova, K. Hensel, E. Spetlikova, L. Sikurova, P. Lukes, *Plasma Process. Polym.* **2013**, *10*, 7.
[11] R. Laurita, D. Barbieri, M. Gherardi, V. Colombo, P. Lukes, *Clin. Plasma Med.* **2015**, *3*, 2.
[12] D. Yan, A. Talbot, N. Nourmohammadi, X. Cheng, J. Canady, J. Sherman, M. Keidar, *Sci. Rep.* **2016**, *5*, 18339.
[13] P. Bruggeman, C. Leys, *J. Phys. D. Appl. Phys.* **2009**, *42*, 53001.
[14] B. R. Locke, P. Lukes, J.-L. Brisset, *Plasma Chemistry and Catalysis in Gases and Liquids* (Eds: V. I. Parvulescu, M. Magureanu, P. Lukes), Wiley-VCH, Weinheim, Germany **2012**, Ch. 6.
[15] P. J. Bruggeman, M. J. Kushner, B. R. Locke, J. G. E. Gardeniers, W. G. Graham, D. B. Graves, R. C. H. M. Hofman-Caris, D. Maric, J. P. Reid, E. Ceriani, D. Fernandez Rivas, J. E. Foster, S. C. Garrick, Y. Gorbanev, S. Hamaguchi, F. Iza, H. Jablonowski, E. Klimova, J. Kolb, F. Krcma, P. Lukes, Z. Machala, I. Marinov, D. Mariotti, S. Mededovic Thagard, D. Minakata, E. C. Neyts, J. Pawlat, Z. Lj. Petrovic, R. Pflieger, S. Reuter, D. C. Schram, S. Schröter, M. Shiraiwa, B. Tarabová, P. A. Tsai, J. R. R. Verlet, T. von Woedtke, K. R. Wilson, K. Yasui, G. Zvereva, *Plasma Sources Sci. Technol.* **2016**, *25*, 53002.
[16] K. Oehmigen, J. Winter, M. Hähnel, C. Wilke, R. Brandenburg, K.-D. Weltmann, T. von Woedtke, *Plasma Process. Polym.* **2011**, *8*, 10.
[17] M. J. Traylor, M. J. Pavlovich, S. Karim, P. Hait, Y. Sakiyama, D. S. Clark, D. B. Graves, *J. Phys. D. Appl. Phys.* **2011**, *44*, 472001.
[18] M. J. Pavlovich, D. S. Clark, D. B. Graves, *Plasma Sources Sci. Technol.* **2014**, *23*, 65036.
[19] J.-L. Brisset, D. Moussa, A. Doubla, E. Hnatiuc, B. Hnatiuc, G. Kamgang Youbi, J.-M. Herry, M. Naïtali, M.-N. Bellon-Fontaine, *Ind. Eng. Chem. Res.* **2008**, *47*, 16.
[20] M. Janda, V. Martišovitš, K. Hensel, Z. Machala, *Plasma Chem. Plasma Process* **2016**, *36*, 3.
[21] A. V. Pipa, S. Reuter, R. Foest, K.-D. Weltmann, *J. Phys. D. Appl. Phys.* **2012**, *45*, 85201.
[22] A. F. H. van Gessel, K. M. J. Alards, P. J. Bruggeman, *J. Phys. D. Appl. Phys.* **2013**, *46*, 265202.
[23] F. Girard, V. Badets, S. Blanc, K. Gazeli, L. Marlin, L. Authier, P. Svarnas, N. Sojic, F. Clément, S. Arbault, *RSC Adv.* **2016**, *6*, 82.
[24] V. N. Vasilets, A. B. Shekhter, *Plasma for Bio-Decontamination, Medicine and Food Security* (Eds: Z. Machala, K. Hensel, Y. Akishev), Springer, Dordrecht, The Nederlands **2012**, Ch. 30.
[25] M. J. Pavlovich, T. Ono, C. Galleher, B. Curtis, D. S. Clark, Z. Machala, D. B. Graves, *J. Phys. D. Appl. Phys.* **2014**, *47*, 505202.
[26] Z. Machala, D. B. Graves, *Trends Biotechnol.* **2017**, *1542*, https://doi.org/10.1016/j.tibtech.2017.07.013
[27] M. J. Pavlovich, Y. Sakiyama, D. S. Clark, D. B. Graves, *Plasma Process. Polym.* **2013**, *10*, 12.
[28] C. A. J. van Gils, S. Hofmann, B. K. H. L. Boekema, R. Brandenburg, P. J. Bruggeman, *J. Phys. D. Appl. Phys.* **2013**, *46*, 175203.
[29] K. Heuer, M. A. Hoffmanns, E. Demir, S. Baldus, C. M. Volkmar, M. Röhle, P. C. Fuchs, P. Awakowicz, C. V. Suschek, C. Opländer, *Nitric Oxide* **2015**, 44.
[30] D. B. Graves, *Plasma Process. Polym.* **2014**, *11*, 12.
[31] K. Oehmigen, M. Hähnel, R. Brandenburg, Ch. Wilke, K.-D. Weltmann, T. von Woedtke, *Plasma Process. Polym.* **2010**, *7*, 3–4.
[32] J. Chauvin, F. Judée, M. Yousfi, P. Vicendo, N. Merbahi, *Sci. Rep.* **2017**, *7*, 1.
[33] C. E. Anderson, N. R. Cha, A. D. Lindsay, D. S. Clark, D. B. Graves, *Plasma Chem. Plasma Process* **2016**, *36*, 6.
[34] K. Wende, P. Williams, J. Dalluge, W. Van Gaens, H. Aboubakr, J. Bischof, T. von Woedtke, S. M. Goyal, K.-D. Weltmann, A. Bogaerts, K. Masur, P. J. Bruggeman, *Biointerphases* **2015**, *10*, 2.
[35] Y. Tian, R. Ma, Q. Zhang, H. Feng, Y. Liang, J. Zhang, J. Fang, *Plasma Process. Polym.* **2015**, *12*, 5.
[36] P. Lu, D. Boehm, P. Cullen, P. Bourke, *Appl. Phys. Lett.* **2017**, *110*, 264102.

[37] V. V. Kovačević, B. P. Dojčinović, M. Jović, G. M. Roglić, B. M. Obradović, M. M. Kuraica, *J. Phys. D. Appl. Phys*. **2017**, *50*, 55205.
[38] V. M. Ivanov, *J. Anal. Chem*. **2004**, *59*, 10.
[39] J. Mack, J. R. Bolton, *J. Photochem. Photobiol. A: Chem*. **1999**, 128.
[40] T. R. Crompton, *Determination of Anions in Natural and Treated Waters*, Spon Press, Taylor & Francis Group, Boca Raton, Florida **2005**.
[41] J.-L. Brisset, J. Pawlat, *Plasma Chem. Plasma Process* **2016**, *36*, 2.
[42] M. J. Pavlovich, H.-W. Chang, Y. Sakiyama, D. S. Clark, D. B. Graves, *J. Phys. D. Appl. Phys*. **2013**, *46*, 145202.
[43] S. Ikawa, K. Kitano, S. Hamaguchi, *Plasma Process. Polym*. **2010**, *7*, 1.
[44] K. Y. Baik, Y. H. Kim, Y. H. Ryu, H. S. Kwon, G. Park, H. S. Uhm, E. H. Choi, *Plasma Process. Polym*. **2013**, *10*, 3.
[45] U. Kogelschatz, *Plasma Phys. Control. Fusion* **2004**, *46*, 12B.
[46] B. Eliasson, M. Hirth, U. Kogelschatz, *J. Phys. D. Appl. Phys*. **1987**, *20*, 11.
[47] M. Magureanu, D. Dobrin, C. Bradu, F. Gherendi, N. B. Mandache, V. I. Parvulescu, *Chemosphere* **2016**, *165*, 507.
[48] D. Ellerweg, A. von Keudell, J. Benedikt, *Plasma Sources Sci. Technol*. **2012**, *21*, 034019.
[49] S. Reuter, J. Winter, S. Iseni, S. Peters, A. Schmidt-Bleker, M. Dünnbier, J. Schäfer, R. Foest, K.-D. Weltmann, *Plasma Sources Sci. Technol*. **2012**, *21*, 3.
[50] W. H. Glaze, *Environ. Sci. Technol*. **1987**, *21*, 3.
[51] C. Wei, F. Zhang, Y. Hu, C. Feng, H. Wu, *Rev. Chem. Eng*. **2016**, *33*, 1.
[52] American Public Health Association, American Water Works Association, Water Environment Federation, *Standard Methods for the Examination of Water and Wastewater*, 20th ed., (Eds: L. S. Clesceri, A. E. Greenberg, A. D. Eaton), United Book Press Inc., Baltimore, USA **2005**.
[53] H. Bader, J. Hoigné, *Water Res*. **1981**, *15*, 4.
[54] C. Yamabe, F. Takeshita, T. Miichi, N. Hayashi, S. Ihara, *Plasma Process. Polym*. **2005**, *2*, 3.
[55] D. Dobrin, C. Bradu, M. Magureanu, N. B. Mandache, V. I. Parvulescu, *Chem. Eng. J*. **2013**, *234*, 389.
[56] J. S. Clements, M. Sato, R. H. Davis, *IEEE Trans. Ind. Appl*. **1987**, *IA-23*, 2.
[57] J. Pawłat, N. Hayashi, C. Yamabe, I. Pollo, *Ozone Sci. Eng*. **2002**, *24*, 3.
[58] J. Pawlat, K. Hensel, *Czech. J. Phys*. **2004**, *54*, S3.
[59] P. Lukes, M. Clupek, V. Babicky, V. Janda, P. Sunka, *J. Phys. D. Appl. Phys*. **2005**, *38*, 3.
[60] S. Burgassi, I. Zanardi, V. Travagli, E. Montomoli, V. Bocci, *J. Appl. Microbiol*. **2009**, *106*, 5.
[61] N. Lu, C. Wang, C. Lou, *J. Soils Sediments* **2017**, *17*, 1.
[62] P. Lukes, A. T. Appleton, B. R. Locke, *IEEE Trans. Ind. Appl*. **2004**, *40*, 1.
[63] J. Pawlat, N. Hayashi, C. Yamabe, *Jpn. J. Appl. Physics, Part 1* **2001**, *40*, 12.
[64] E. Marotta, M. Schiorlin, X. Ren, M. Rea, C. Paradisi, *Plasma Process. Polym*. **2011**, *8*, 9.
[65] M. Janda, Z. Machala, L. Dvonč, D. Lacoste, C. O. Laux, *J. Phys. D. Appl. Phys*. **2015**, *48*, 035201.
[66] M. Janda, . V. Martišovitš, K. Hensel, L. Dvonč, Z. Machala, *Plasma Sources Sci. Technol*. **2014**, *23*, 065016.
[67] M. Janda, V. Martišovitš, Z. Machala, *Plasma Sources Sci. Technol*. **2011**, *20*, 035015.
[68] B. Pongrác, H.-H. Kim, N. Negishi, Z. Machala, *Eur. Phys. J. D* **2014**, *68*, 8.
[69] B. Pongrác, H.-H. Kim, M. Janda, V. Martišovitš, Z. Machala, *J. Phys. D. Appl. Phys*. **2014**, *47*, 315202.
[70] K. Hensel, K. Kučerová, B. Tarabová, M. Janda, Z. Machala, K. Sano, C. T. Mihai, M. Ciorpac, L. D. Gorgan, R. Jijie, V. Pohoata, I. Topala, *Biointerphases* **2015**, *10*, 2.
[71] J. Orphal, *J. Photochem. Photobiol. A: Chem*. **2003**, *157*, 2–3.
[72] C. O. Laux, T. G. Spence, C. H. Kruger, R. N. Zare, *Plasma Sources Sci. Technol*. **2003**, *12*, 2.
[73] U. Fantz, *Plasma Sources Sci. Technol*. **2006**, *15*, 4.
[74] Z. Machala, M. Janda, K. Hensel, I. Jedlovský, L. Leštinská, V. Foltin, V. Martišovitš, M. Morvová, *J. Mol. Spectrosc*. **2007**, *243*, 2.
[75] G. M. Eisenberg, *Ind. Eng. Chem. Anal. Ed*. **1943**, *15*, 5.
[76] D. L. Rusterholtz, D. A. Lacoste, G. D. Stancu, D. Z. Pai, C. O. Laux, *J. Phys. D. Appl. Phys*. **2013**, *46*, 464010.
[77] D. B. Graves, *J. Phys. D. Appl. Phys*. **2012**, *45*, 263001.
[78] J.-L. Brisset, E. Hnatiuc, *Plasma Chem. Plasma Process* **2012**, *32*, 4.
[79] B. Tarabová, K. Tarabová, K. Hensel, L. Šikurová, Z. Machala, *Book of Contributions, 14th International Symposium on High Presure Low Temperature Plasma Chemistry* (Eds: R. Brandenburg, L. Stolenwerk), INP Greifswald and IfP Greifswald, Greifswald, Germany **2014**.

How to cite this article: Tarabová B, Lukeš P, Janda M, Hensel K, Šikurová L, Machala Z. Specificity of detection methods of nitrites and ozone in aqueous solutions activated by air plasma. *Plasma Process Polym*. 2018;**15**:e1800030. https://doi.org/10.1002/ppap.201800030

APPENDIX

Table A1 Summary of the used abbreviations

Aqueous solutions	
PB	Phosphate buffer
PAPB	Plasma activated phosphate buffer
W	Water
PAW	Plasma activated water
sPAW	Synthetic plasma activated water
Scavengers of reactive species	
CAT	Catalase
MAN	Mannitol
SA	Sodium azide
Other abbreviations	
ES	Electrospray
HPLC	High performance liquid chromatography
IC	Ion chromatography
OES	Optical emission spectroscopy
RONS	Reactive oxygen and nitrogen species
TS	Transient spark